Stoch Environ Res Risk Assess (2009) 23:613–620
DOI 10.1007/s00477-008-0246-2

ORIGINAL PAPER

Uncertainty propagation of hydrodispersive transfer in an aquifer: an illustration of one-dimensional contaminant transport with slug injection

David Ching-Fang Shih · Yue-Gau Chen · Gwo-Fong Lin · Yih-Min Wu

Published online: 14 June 2008

Abstract It is evident that the hydrodynamic dispersion coefficient and linear flow velocity dominate solute transport in aquifers. Both of them play important roles characterizing contaminant transport. However, by definition, the parameter of contaminant transport cannot be measured directly. For most problems of contaminant transport, a conceptual model for solute transport generally is established to fit the breakthrough curve obtained from field testing, and then suitable curve matching or the inverse solution of a theoretical model is used to determine the parameter. This study presents a one-dimensional solute transport problem for slug injection. Differential analysis is used to analyze uncertainty propagation, which is described by the variance and mean. The uncertainties of linear velocity and hydrodynamic dispersion coefficient are, respectively, characterized by the second-power and fourth-power of the length scale multiplied by a lumped relationship of variance and covariance of system parameters, i.e. the Peclet number and arrival time of maximum concentration. To validate the applicability for evaluating variance propagation in one-dimensional solute transport, two cases using field data are presented to demonstrate how parametric uncertainty can be caught depending on the manner of sampling.

Keywords Uncertainty · Differential analysis · Groundwater · Solute transport · Dispersion coefficient · Slug injection

D. C.-F. Shih · Y.-G. Chen · Y.-M. Wu
Department of Geosciences, National Taiwan University, Taipei, Taiwan, ROC

G.-F. Lin
Department of Civil Engineering, National Taiwan University, Taipei, Taiwan, ROC

D. C.-F. Shih
Institute of Nuclear Energy Research, AEC, Lungtan, Taiwan, ROC

D. C.-F. Shih (✉)
P·O. Box 3-7, Lungtan 32546, Taiwan, ROC
e-mail: cfshih@iner.gov.tw

1 Introduction

Groundwater moves at rates that are both greater and less than the average linear velocity. On the macroscopic scale, the domain includes a sufficient volume that the effects of individual pores are averaged (Bear 1972). As fluid moves through pores, it moves faster in pore centers than along the edges. Some of the fluid particles will travel along longer flow paths in the porous media than other particles over the same linear distance. Some pores also are larger than others, which allow the fluid flowing through these pores to move faster. If all groundwater containing a solute were to travel at exactly the same rate, it would displace water that does not contain the solute and create an abrupt interface between the two fluids. However, because the solute-containing water entering the system does not all travel at the same velocity, mixing occurs along the flow path and mechanical dispersion is observed (Fetter 1999). The hydrodynamic dispersion coefficient comprises both mechanical dispersion and effective diffusion and it dominates the solute transport in an aquifer along with the linear flow velocity. Practically, from the view point of site characterization, a detailed flow field with boundary conditions needs to be investigated. Fetter (1999) collects a few well-known and traditional studies of solute transport, most of which are clear in theory and easy to follow. It is

generally known that reasonable interpretation of tracer testing results is critical for characterizing a site. A slug of contamination is instantaneously injected into a uniform, one-dimensional flow field, and will pass through the aquifer as a concentration pulse. Conceptual models can be developed to preliminarily provide effective field tests for assessing hydrodispersive conditions. Sauty (1980) proposed a dimensionless representation for one-dimensional solute transport using the interpretation of Peclet number (P_e) for such idea. The method and procedure are quite easy and effective, but unsuitable curve matching and the selection of peak value frequently occur. It was found that in many applications type curve matching for the observation and pre-defined conceptual model, more or less, cannot be well matched, e.g. Perkins and Johnson (1963), Picken and Grisak (1981), Throne and Newcomer (1992), and Leveinen (2000); this perhaps due to the unknown or the uncertainty regarding the system. In general, one will use the limited data and information at that time to set up suitable and pre-defined model in most cases. Uncertainty analysis is one of the works to realize the gap between the observation and real system even the latter generally cannot be well decided according the field data. This research demonstrate the propagation of parametric uncertainty using differential analysis illustrating one-dimensional contaminant transport using slug injection proposed by Sauty (1980). It provides an effective procedure for the assessment of propagation of uncertainty for the domain with limited data. Conceptually, variance is a measure of deviation from its mean value, and can be used to identify the uncertainty of models or parameters in the absence of sufficient data. The study also demonstrates a parametric analysis method to verify the propagation of model variance and to identify the nature of its uncertainty.

Measurement of uncertainty and parameter importance has been analyzed for the corrosion depth of spent nuclear fuel canisters by using differential analysis. (Shih et al. 2002; Shih and Lin 2006) Uncertainty analysis of radioactive nuclide transport for a one-dimensional single fracture has also been studied. (Shih 2004) First-order differential analysis was applied to develop the analytical form of the expected value and variance for the contaminant transport equation by considering uncertainty of the dispersion coefficient and retardation factor. In that study, only the mean value and variance of the system output were considered to evaluate parameter uncertainty and its importance to the problem. Differential analysis has been also reviewed and used in other relevant studies (NRC 1989; Shih and Lin 2006). Many other methods for conducting parametric uncertainty and derivative sensitivity are found in earlier works, but are beyond the scope of this study (Myers 1971; Schaibly and Shuler 1973; Gardner and O'Neill 1983).

2 Analytical system of contaminant transport

The derivation of the advection-dispersion equation is partly based on work by Freeze and Cherry (1979), Bear (1972), and Ogata (1970). The working assumptions are that the porous medium is homogeneous, isotropic, saturated and that flow conditions are such that Darcy's law is valid. The conservation of mass of solute flux into and out of a small representative elementary volume of the porous media is considered. In a homogeneous medium, because the coefficient of hydrodynamic dispersion is dominated in the flow direction by the average linear flow velocity, v_x, the flow is uniform in space. A conceptual model of solute transport for a slug injection test is shown in Fig. 1. It suggests the studied model is one-dimensional contaminant transport of solute in a homogeneous and isotropic porous media; Fetter (1999) described that

$$D_L \frac{\partial^2 C}{\partial x^2} - v_x \frac{\partial C}{\partial x} = \frac{\partial C}{\partial t} \tag{1}$$

where C: solute concentration (M^3/L); D_L: hydrodynamic dispersion coefficient parallel to the principal direction of flow (longitudinal) (L^2/T); v_x: flow velocity (L/T); x: axis of coordinate in one-dimensional transport direction (L); and t: time (T) (Fig. 1).

As is generally known, the mass transport equation uses hydrodynamic dispersion, which is the combination of mechanical dispersion and diffusion. It is possible to evaluate the relative contribution of mechanical dispersion and diffusion to solute transport. Using the Peclet number, which is a dimensionless number relating the effectiveness of mass transport by advection to the effectiveness of mass transport by either dispersion or diffusion (Fetter 1999). The Peclet number has the form $v_x\, L/D_L$, where L is the characteristic flow length. At zero flow velocity, D_L is equal to D^*, since

$$D_L = \alpha_L v_x + D* \tag{2}$$

where α_L: longitudinal dynamic dispersivity (L), and D^*: the effective diffusion coefficient (L^2/T) (De Josselin De John 1958).

A mass of solute is instantaneously introduced into the aquifer at time t_0 over the interval $x = 0 + a$. The resulting initial concentration is C_0. Groundwater advection carries the mass of solute with it. In the process, the solute slug spreads out, so that the maximum concentration decreases with time. The diffusion model of hydrodynamic dispersion predicts that the concentration curves have a Gaussian distribution described by a mean and variance. (Fetter 1999) Hence, the coefficient of longitudinal hydrodynamic dispersion can be also defined as

$$D_L = \frac{\sigma_L^2}{2t} \tag{3}$$

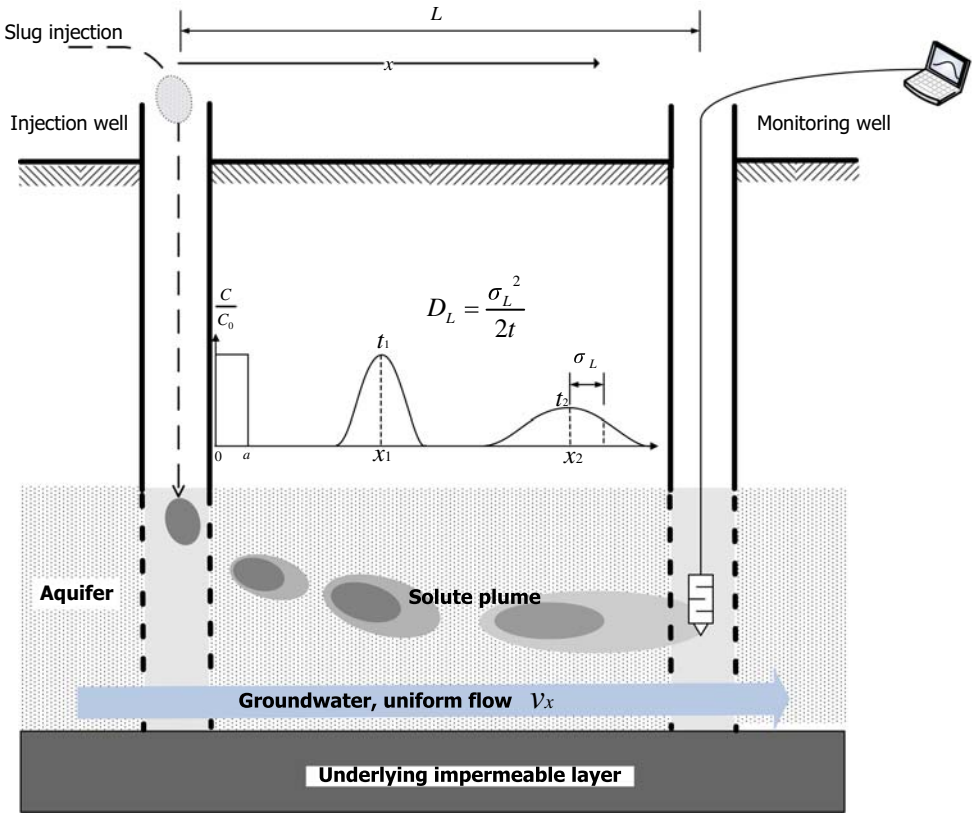

Fig. 1 Conceptual model of a one-dimensional flow field and solute transport using slug injection; in which the spreading breakthrough curve is redrawn after Fetter (1999, p. 54)

where $\sigma_L{}^2$: variance of the longitudinal spreading of the plume. However, the typical representation of Eq. (3) cannot be evaluated using field test data.

If a slug of contamination is instantaneously injected into a uniform, one-dimensional flow field, it passes through the aquifer as a pulse with a peak concentration, $C_{\max}$, at some time after injection, $t_{\max}$. The solution of Eq. (1) under such conditions (Sauty 1980) is, in dimensionless form,

$$C_R(t_R, P_e) = \frac{H}{(t_R)^{1/2}} \exp\left(-\frac{P_e}{4t_R}(1-t_R)^2\right) \tag{4}$$

with

$$H = (t_{R\max})^{1/2} \exp\left(-\frac{P_e}{4t_{R\max}}(1-t_{R\max})^2\right) \tag{5}$$

and where

$$t_{R\max} = \left(1+P_e^{-2}\right)^{1/2} - P_e^{-1} \tag{6}$$

is the dimensionless time at which peak concentration occurs, and

$$C_R = \frac{C}{C_{\max}} \tag{7}$$

$$t_R = \frac{v_x t}{L} \tag{8}$$

$$P_e = \frac{v_x L}{D_L} \tag{9}$$

Figure 2 shows dimensionless curves for a slug injected into a uniform, one-dimensional flow field for several Peclet numbers. It is found that the time for the peak concentration $C_R(C/C_{\max})$ increases with the Peclet number up to a bounding value at $t_R = 1$. Breakthrough becomes more symmetric with increasing values of P_e.

As the conceptual model and procedure described in Eqs. (1)–(9), a one-dimensional flow field is created where the distance from the injection well to the observation well is small, such that the effect of decreasing pressure head on groundwater flow can be neglected. Solute concentration can be observed at a downstream observation well. One can prepare plots (Fig. 2) for C_R versus t_R for different P_e numbers. Acquiring the variation of C versus t from the field test, it needs to plot a C–t curve. A specific P_e number is chosen that best matches the C_R–t_R and C–t curve. Once $t_{\max}$ is determined for the arrival time related to peak concentration, v_x can be calculated using Eq. (8), i.e. $v_x = t_{R\max} L/t_{\max}$, where $t_{R\max}$ is estimated by Eq. (6) using the selected P_e. The hydrodynamic dispersion coefficient D_L can be determined by Eq. (9). Using the above procedure, it is straightforward to determine the hydrodynamic dispersion coefficient from the field test data.

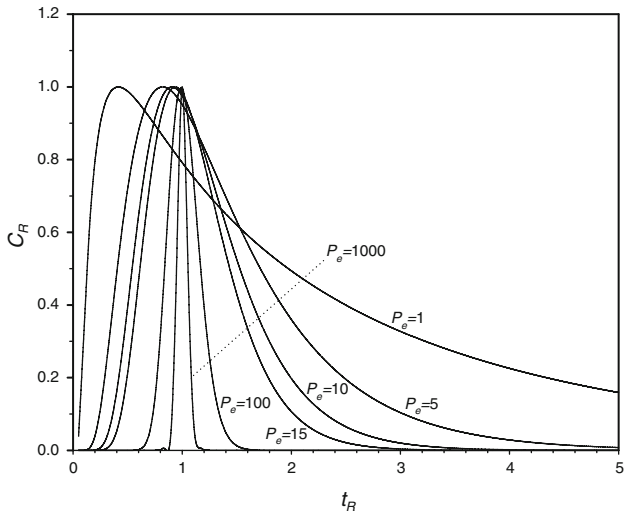

Fig. 2 Dimensionless curve for a one-dimensional flow field and solute transport using slug injection. It can be found that the time for the dimensionless peak concentration C_R ($C/C_{\max}$) to occur increases with the Peclet number up to a bounding value at dimensionless time $t_R = 1$. Breakthrough becomes more symmetric with increasing P_e. Theoretical source: Sauty (1980)

3 Differential analysis for uncertainty assessment

It assumes that the mean value and variance constitute the statistical model of the system. Basically, mean, variance and covariance can be, respectively, expressed as

$$E(p_i) = m^{-1}\sum_{k=1}^{m} p_{ik} \tag{10}$$

$$\mathrm{Var}(p_i) = (m-1)^{-1}\sum_{k=1}^{m}(p_{ik} - E(p_i))^2 \tag{11}$$

$$\mathrm{Cov}(p_i, p_j) = (m-1)^{-1}\sum_{k=1}^{m}(p_{ik} - E(p_i))(p_{jk} - E(p_j)) \tag{12}$$

where m: the sample size, p_i and p_j are independent parameter variables, and k: running index for samples.

The differential analysis uses the Taylor-series to approximate the system model under consideration. (NRC 1989) It is assumed that the model under consideration can be represented by a function of the form (NRC 1989; Shih and Lin 2006)

$$y = f(p_1, p_2, \ldots, p_n) = y(\mathbf{p}). \tag{13}$$

Base values and ranges are selected for the input variables p_i, $i = 1, 2,\ldots,n$. The base values can be represented by the vector

$$\mathbf{p_0} = [p_{10}, p_{20}, \ldots, p_{n0}] \tag{14}$$

Using the multidimensional Taylor-series expansion, the first-order approximation to y is

$$y(\mathbf{p}) \cong y(\mathbf{p_0}) + \sum_{i=1}^{n}\frac{\partial f(\mathbf{p_0})}{\partial p_i}(p_i - p_{i0}) \tag{15}$$

In essence, uncertainty analysis is an evaluation of the propagation of the mean and variance of input parameters to system response. Respectively, mean and variance of the system output y can be estimated by

$$E(y) \cong y(\mathbf{p_0}) + \sum_{i=1}^{n}\frac{\partial f(\mathbf{p_0})}{\partial p_i}E(p_i - p_{i0}) = y(\mathbf{p}_0) \tag{16}$$

and

$$\mathrm{Var}(y) \cong \sum_{i=1}^{n}\left(\frac{\partial f(\mathbf{p_0})}{\partial p_i}\right)^2 \mathrm{Var}(p_i) + 2\sum_{i=1}^{n}\sum_{j=i+1}^{n}\left[\frac{\partial f(\mathbf{p_0})}{\partial p_i}\right]\left[\frac{\partial f(\mathbf{p_0})}{\partial p_j}\right]\mathrm{Cov}(p_i, p_j) \tag{17}$$

In Eq. (16), $E(p_i - p_{i0}) = E(p_i) - p_{i0} = 0$, where p_{i0} is constant and it suggests the expectation value of the sample always equal to its base value of sample. The mean is the average value for a set of data, while variance is a measure of deviation from the mean. In nature, parameter variance can propagate to system output according to the relationship of Eq. (17). The resultant variance of the output response is dependent on the variance and covariance of the system inputs. Methodology reviews and applications for differential analysis may be found in earlier studies (NRC 1989; Shih et al. 2002; Shih 2004; Shih and Lin 2006).

4 Uncertainty analysis

A one-dimensional slug injection tracer test in a gravel aquifer was conducted to demonstrate the propagation of parametric uncertainty. Rhodamine-WT (20% active) was used as the tracer, and a background level was designated as 0.2 ppb. Excitation and emission wavelengths for Rhodamine-WT were selected at 546 and 590 nm, respectively, with a linear detection range of 0.1–100 ppb. Fully penetrating wells were drilled in the aquifer. The aquifer has a thickness of 20 m with a relatively impermeable layer at 24 m, and an aquifer table 3.5 meters beneath the ground surface. The distance (L) between injection and observation wells is 21.87 m. Breakthrough curves for $P_e = 4$ to 15 are shown in Fig. 3. In the deterministic application, one often chooses the type curve which they feel "the best" and conduct the calculation of the parameter in the following. In this research, Fig. 3 shows that the fitted solution does not come close to the observation data but it seems to fall into the range for $P_e = 4$ through 15. It reveals some mechanism missing the conceptual model and gives rise the problem for the unknown sources of model uncertainty. However, for lake of the field data, it still suggests hydrodispersive condition can

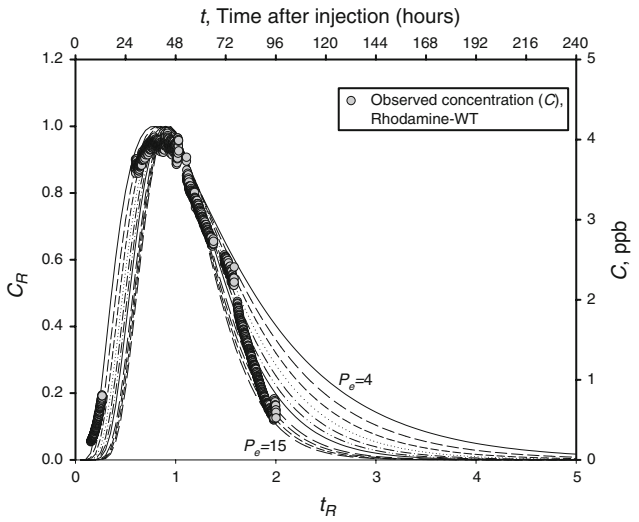

Fig. 3 Breakthrough curve versus dimensionless curve of one-dimensional flow field and solute transport using slug injection. The tracer test was conducted using Rhodamine-WT water tracer with 0.2 ppb background level. *Plot* is sketched for all possible values to demonstrate the complete analysis picture

be assessed using Eqs. (4)–(9), and (16)–(17), to demonstrate the parametric uncertainty in sampling for preliminary assessment. Recall that the specific P_e number is determined by the best matching between C_R–t_R and C–t curves. Once $t_{\max}$ is determined for the time related to peak concentration, the groundwater velocity (v_x) and hydrodynamic dispersion coefficient (D_L) can be calculated using Eqs. (8) and (9). However, there is a problem in that the selection of P_e from the matching curve (Fig. 4) is rather arbitrary and subjective, and it can also be arbitrary to pick the $t_{\max}$ in the time from 36 to 48 h in Fig. 5. What is the uncertainty in such a process, and how can one address the variability for determining v_x and D_L? Note that v_x and D_L are system outputs described as Eqs. (8) and (9), respectively. By incorporating Eqs. (8) and (9), the expected value or the mean for v_x and D_L can be derived using Eq. (16), and are

$$E(v_x) = \frac{E(t_{R\max})L}{E(t_{\max})} \tag{18}$$

$$E(D_L) = \frac{E(t_{R\max})L^2}{E(t_{\max})E(P_e)} \tag{19}$$

In the same manner, variances of the output are

$$\begin{aligned}\mathrm{Var}(v_x) = {} & \left(\frac{L}{E(t_{\max})}\right)^2 \mathrm{Var}(t_{R\max}) + \left(\frac{-E(t_{R\max})L}{E(t_{\max})^2}\right)^2 \\ & \times \mathrm{Var}(t_{\max}) + 2\left(\frac{L}{E(t_{\max})}\right)\left(\frac{-E(t_{R\max})L}{E(t_{\max})}\right) \\ & \times \mathrm{Cov}(t_{R\max}, t_{\max})\end{aligned} \tag{20}$$

and

$$\begin{aligned}\mathrm{Var}(D_L) = {} & \left(\frac{L^2}{E(t_{\max})E(P_e)}\right)^2 \mathrm{Var}(t_{R\max}) + \left(\frac{-E(t_{R\max})L^2}{E(t_{\max})^2E(P_e)}\right)^2 \\ & \times \mathrm{Var}(t_{\max}) + \left(\frac{-E(t_{R\max})L^2}{E(t_{\max})E(P_e)^2}\right)^2 \mathrm{Var}(P_e) \\ & + 2\left(\frac{L^2}{E(t_{\max})E(P_e)}\right)\left(\frac{-E(t_{R\max})L^2}{E(t_{\max})^2E(P_e)}\right) \\ & \times \mathrm{Cov}(t_{R\max}, t_{\max}) + 2\left(\frac{L^2}{E(t_{\max})E(P_e)}\right) \\ & \times \left(\frac{-E(t_{R\max})L^2}{E(t_{\max})E(P_e)^2}\right)\mathrm{Cov}(t_{R\max}, p_e) \\ & + 2\left(\frac{-E(t_{R\max})L^2}{E(t_{\max})^2E(P_e)}\right)\left(\frac{-E(t_{R\max})L^2}{E(t_{\max})E(P_e)^2}\right) \\ & \times \mathrm{Cov}(t_{\max}, P_e)\end{aligned} \tag{21}$$

Most notably, P_e is chosen independently for matching the C_R–t_R and C–t curves and is computed as Eq. (6). The $t_{\max}$ are read independently as many possible values from the breakthrough curve. Consequently, it is suggested that $t_{R\max}$ is also uncorrelated to $t_{\max}$ due to Eq. (6). By dropping the covariance term related to P_e versus $t_{\max}$ and $t_{R\max}$ versus $t_{\max}$, Eqs. (20) and (21) can be rewritten as

$$\begin{aligned}\mathrm{Var}(v_x) = {} & L^2\left(\mathrm{Var}(t_{R\max}) + \frac{E(t_{R\max})^2}{E(t_{\max})^2}\mathrm{Var}(t_{\max})\right) \\ & \times E(t_{\max})^{-2} = L^2\phi(t_{\max}, t_{R\max})\end{aligned} \tag{22}$$

$$\begin{aligned}\mathrm{Var}(D_L) = {} & L^4\left(\mathrm{Var}(t_{R\max}) + \frac{E(t_{R\max})^2}{E(t_{\max})^2}\mathrm{Var}(t_{\max}) + \frac{E(t_{R\max})^2}{E(P_e)^2}\right. \\ & \left. \times \mathrm{Var}(P_e) - \frac{2E(t_{R\max})}{E(P_e)}\mathrm{Cov}(t_{R\max}, P_e)\right) \\ & \times E(t_{\max})^{-2}E(P_e)^{-2} \\ = {} & L^4\Phi(t_{\max}, P_e, t_{R\max})\end{aligned} \tag{23}$$

$E()$ denotes the expected value (or the mean) for Eq. (20) through to (23), which can be the base value using the sample mean of the parameter (NRC 1989). Var() and Cov() indicate variance and covariance, respectively, and can be calculated from the sampling experiments acquiring $t_{\max}$ and P_e, and calculated $t_{R\max}$. ϕ and Φ are functional representations as shown in the Eqs. (22) and (23), respectively.

The coefficient of variation (CV) is a normalized measure of dispersion of a probability distribution. It is defined as the ratio of the standard deviation to the mean. This is only defined for non-zero mean, and is most useful for variables that are always positive. It is often reported as a percentage (%) by multiplying the above calculation by

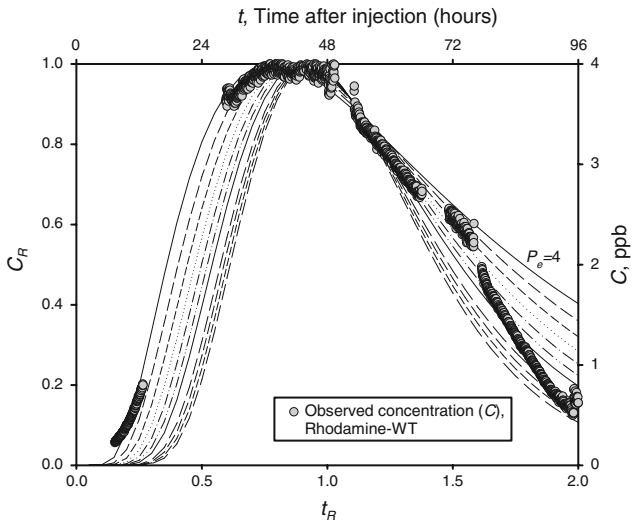

Fig. 4 Same as Fig. 3. Breakthrough curve versus dimensionless curve of one-dimensional flow field and solute transport. *Plots* are emphasized to show the curve matching for selecting suitable P_e

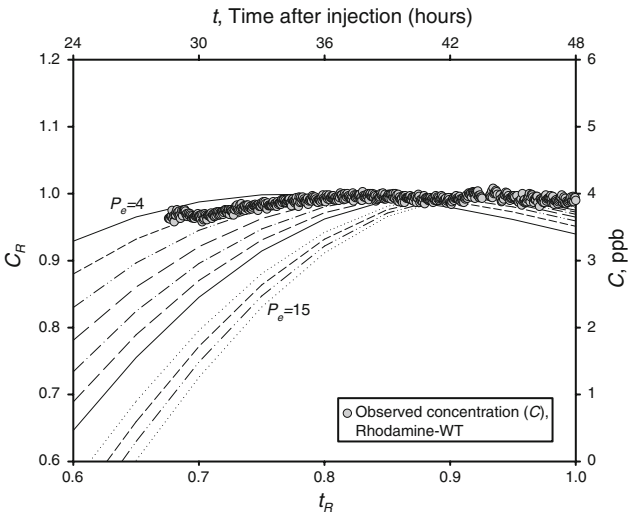

Fig. 5 Same as Fig. 3. Breakthrough curve versus dimensionless curve of one-dimensional flow field and solute transport. *Plots* are emphasized to show the arrival time of maximum concentration, used for picking possible arrival times of peak concentration

100. It suggests that system output defined in Eqs. (22) and (23) are population estimate, then, simplify the CV as

$$\mathrm{CV} = \frac{\sigma}{E(y)} = \frac{\sqrt{\mathrm{Var}(y)}}{E(y)} \tag{24}$$

5 Discussion

It is found that the experimental mean value of v_x and D_L as shown in Eqs. (18) and (19) are dependent on the mean values of P_e, $t_{R\max}$ and $t_{\max}$, and also relate to the first-power and second-power of length scale (L), respectively. The variables ϕ and Φ are defined as lumped parameters of the mean value, variance and covariance associated with P_e, $t_{R\max}$ and $t_{\max}$. The variance of v_x and D_L are then characterized by $L^2\phi$ and $L^4\Phi$, respectively. The more centralized the distributions of sampling P_e, $t_{R\max}$ and $t_{\max}$ are, the less uncertainty of v_x and D_L if the length scale is unchanged. Note that the uncertainty of v_x and D_L will be amplified by the second-power and fourth-power of the distance L, respectively. This implies that the farther away from the injected well, the greater the uncertainty in v_x and D_L will be. Table 1 shows the case 1 of experimental sampling for P_e, $t_{R\max}$ and $t_{\max}$, for which $t_{R\max}$ is computed using Eq. 6. Possible P_e are selected arbitrarily by curve matching $t_{\max}$ (Fig. 3), while $t_{\max}$ values are taken from the peak values of the field test data (Fig. 4). Resultant expected value, variance, and covariance are calculated (Table 2); scaled variances by the expected value are also shown in Table 3. It shows that output variance for D_L is 7.7% of the mean and 0.1% for v_x. For the case 2, the most centralized P_e and the widest of samples $t_{\max}$ in the peak range are selected (Table 4). Clearly, the output variations of D_L and v_x are significantly reduced, even though $t_{\max}$ is more uncertain than in case 1 (Tables 5, 6; Fig. 6). Experimental sampling for choosing P_e and $t_{\max}$ appears to be very important as the uncertainty propagation clearly exists. The existence of parametric uncertainty in environmental modeling applications is often neglected. As the above stochastic analysis derived from the deterministic method of Sauty (1980), this work substantially demonstrates the propagation of parametric uncertainty for a one-dimensional tracer test.

6 Conclusion

It illustrates the uncertainty of parameter sampling for hydrodispersive transfer in an aquifer using the dimensionless equations for a slug of contamination instantaneously injected into a uniform one-dimensional flow field. In the deterministic application, one often

Table 1 Case 1: parameter selection for P_e and $t_{\max}$

P_e	4, 5, 6, 7
$t_{R\max}$	0.781, 0.820, 0.847, 0.867
L (m)	21.870
$t_{\max}$ (h)	38.485, 38.518, 38.552, 38.585, 38.618, 38.652, 38.685, 38.718, 38.752, 38.785, 38.818, 38.852

The value of $t_{R\max}$ is computed from Eq. (6) and L is the scale length of the field test domain. In comparison to case 2, P_e is subjectively selected and is more uncertain, and a limited number of $t_{\max}$ values are chosen from the recorded field test data

Table 2 Case 1: expected value, variance, and covariance based on the system parameter data in Table 1

Expected value	$E(P_e)$	$E(t_{R\max})$, h	$E(t_{\max})$, h	$E(v_x)$, m/h	$E(D_L)$, m^2/h
	5.500E + 00	8.288E-01	3.867E + 01	4.687E-01	1.864E + 00
Variance	$\mathrm{Var}(P_e)$	$\mathrm{Var}(t_{R\max})$, h^2	$\mathrm{Var}(t_{\max})$, h^2	$\mathrm{Var}(v_x)$, (m/h)^2	$\mathrm{Var}(D_L)$, (m^2/h)^2
	1.667E + 00	1.402E-03	1.444E-02	4.505E-04	1.439E-01
Covariance	$\mathrm{COV}(t_{R\max}, P_e)$, h				
	3.586E-02				

Table 3 Case 1: output uncertainty of system parameters, which is characterized by the ratio of variance to expectation and based on the results shown in Table 2

Terms	Value	CV (%)
$\mathrm{Var}(P_e)/E(P_e)$	3.030E-01	30.303
$\mathrm{Var}(t_{R\max})/E(t_{R\max})$	1.691E-03	0.169
$\mathrm{Var}(t_{\max})/E(t_{\max})$	3.735E-04	0.037
$\mathrm{Var}(v_x)/E(v_x)$	9.611E-04	0.096
$\mathrm{COV}(t_{R\max}, P_e)/(E(t_{R\max}) \times E(P_e))$	7.867E-03	0.787
$\mathrm{Var}(D_L)/E(D_L)$	7.719E-02	7.718

Table 4 Case 2: parameter selection for P_e and $t_{\max}$

P_e	5.1, 5.2, 5.3, 5.4, 5.5, 5.6, 5.7, 5.8, 5.9, 6.0
$t_{R\max}$	0.823, 0.826, 0.829, 0.832, 0.835, 0.837, 0.840, 0.842, 0.845, 0.847
L (m)	21.870
$t_{\max}$ (h)	38.351, 38.385, 38.418, 38.452, 38.485, 38.518, 38.552, 38.585, 38.618, 38.652, 38.685, 38.718, 38.752, 38.785, 38.818, 38.852, 38.885, 38.918, 38.952, 38.985, 39.018, 39.052, 39.085, 39.118, 39.152, 39.185, 39.218, 39.252, 39.285, 39.318

The parameter $t_{R\max}$ is computed from Eq. (6) and L is the scale length of the field test domain. In comparison to case 1, P_e is selected more precisely for the possible curve, and there are more values of $t_{\max}$

determines "the best" type curve matching as they felt and conduct the calculation of the parameter in the following. For lake of the field data, preliminary assessment of hydrodispersive condition can still be determined using in the conventional field work with type curve matching. In basic, uncertainty as demonstrated by the variance is a measure of deviation from the mean value while stochastic measurements of parametric uncertainty propagation can be analyzed using differential analysis. In this study, the uncertainty of linear flow velocity and hydrodynamic dispersion coefficient can be, respectively, characterized by the second-power and fourth-power of the length scale multiplied by a lumped parameter consisting of the variance and covariance of system parameters. Experimental sampling for choosing the arrival time of maximum concentration from field test data and selecting the matched curves appear to be very important due to existing natural uncertainty. It introduces a method for studying uncertainty propagation in a model and demonstrates its applications using real field data. Two realistic cases are presented comparing propagation of parametric uncertainty through experienced sampling. Note that many environmental systems exhibit a variety of uncertain phenomena; variations of system output resulting from variations of input parameters is one of the most important phenomena.

Table 6 Case 2: output uncertainty of system parameters, which is characterized by the ratio of variance to expectation and using the results from Table 5

Terms	Value	CV (%)
$\mathrm{Var}(P_e)/E(P_e)$	1.652E-02	1.652
$\mathrm{Var}(t_{R\max})/E(t_{R\max})$	7.899E-05	0.008
$\mathrm{Var}(t_{\max})/E(t_{\max})$	2.217E-03	0.222
$\mathrm{Var}(v_x)/E(v_x)$	7.135E-05	0.007
$\mathrm{COV}(t_{R\ \max}, P_e)/(E(t_{R\ \max}) \times E(P_e))$	4.030E-03	0.403
$\mathrm{Var}(D_L)/E(D_L)$	4.769E-04	0.048

Table 5 Case 2: expected value, variance, and covariance using the system parameter data from Table 4

Expected value	$E(P_e)$	$E(t_{R\max})$, h	$E(t_{\max})$, h	$E(v_x)$, m/h	$E(D_L)$, m^2/h
	5.550E + 00	8.356E-01	3.884E + 01	4.706E-01	1.854E + 00
Variance	$\mathrm{Var}(P_e)$	$\mathrm{Var}(t_{R\max})$, h^2	$\mathrm{Var}(t_{\max})$, h^2	$\mathrm{Var}(v_x)$, (m/h)^2	$\mathrm{Var}(D_L)$, (m^2/h)^2
	9.167E-02	6.600E-05	8.611E-02	3.357E-05	7.473E-03
Covariance	$\mathrm{COV}(t_{R\max}, P_e)$, h				
	2.212E-03				

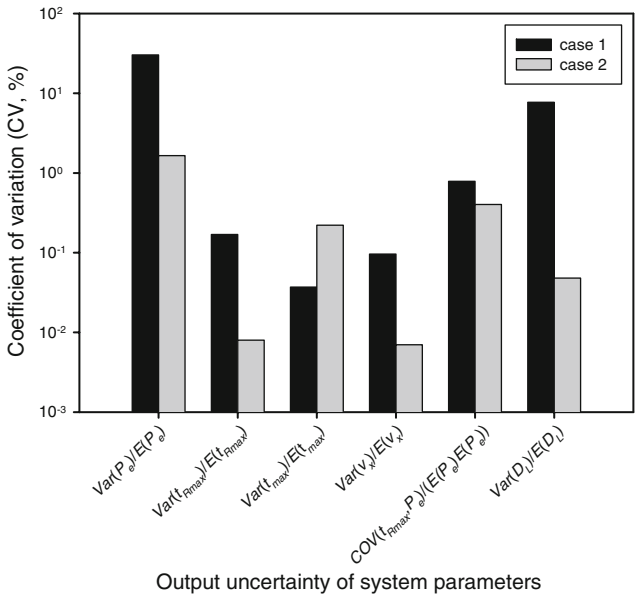

Fig. 6 CV of the input parameters comparing different sampling manner. Case 1 and 2 denote the reference and alternative case, respectively. Case 2 is represented as an improved result, even though it uses a wider range of arrival time of maximum concentration [see $\mathrm{Var}(t_{\max})/E(t_{\max})$]

Acknowledgments The support of the Department of Geosciences of National Taiwan University and the Institute of Nuclear Energy Research (AEC) of Taiwan are gratefully acknowledged.

References

Bear J (1972) Dynamics of fluids in porous media. American Elsevier Publishing Company, New York

De Josselin De John G (1958) Longitudinal and transverse diffusion in granular deposits. Trans Am Geophys Union 39(1):67

Fetter CW (1999) Contaminant Hydrogeology. Prentice Hall, Englewood Cliffs

Freeze RA, Cherry JA (1979) Groundwater. Prentice Hall, Englewood Cliffs

Gardner RH, O'Neill RV (1983) Parameter uncertainty and model predictions: a review of Monte Carlo results. In: Beck MB, Van Straten G (eds) In uncertainty, forecasting of water quality. Springer, New York

Leveinen J (2000) Composite model with fractional flow dimensions for well test analysis in fractured rocks. J Hydrol 234(3–4):116–141

Myers RH (1971) Response surface methodology. Allyn and Bacon, Boston

NRC (1989) A review of techniques for propagating data and parameter uncertainties in high-level radioactive waste repository performance waste repository performance assessment models. NUREG/CR-5393 (SAND89-1432), Nuclear Regulatory Commission, USA

Ogata A (1970) Theory of dispersion in a granular medium. US Geological Survey Professional Paper 411-I

Perkins TK, Johnson OC (1963) A review of diffusion and dispersion in porous media. Soc Pet Eng J 3:70–84

Picken JF, Grisak GE (1981) Scale-dependent dispersion in a stratified granular aquifer. Water Resour Res 17(4):1191–1211

Sauty JP (1980) An analysis of hydrodispersive transfer in aquifers. Water Resour Res 16(1):145–158

Schaibly JH, Shuler KE (1973) Study of the sensitivity of coupled reaction systems to uncertainties in rate coefficients, II. Application. J Chem Phys 59:3879–3888

Shih DCF (2004) Uncertainty analysis: one-dimensional radioactive nuclide transport in a single fractured media. Stoch Environ Res Risk Assess 18:198–204

Shih DCF, Chuang WS, Chang SS, Kuo MC, Lin GF (2002) Uncertainty analysis for corrosion depth of nuclear spent fuel canister, Waste Management'02, Session 39B, paper #575, 24–29 February 2002, Tucson, AZ/USA

Shih DCF, Lin GF (2006) Uncertainty and importance assessment using differential analysis: an illustration of corrosion depth of spent nuclear fuel canister. Stoch Environ Res Risk Assess 20:291–295

Throne PD, Newcomer DR (1992) Summary and evaluation of available hydraulic property data for the Hanford site unconfined aquifer system. US DOS DE-AC06-76RLO 1830, Pacific Northwest Laboratory, PNL-8337/UC-402,403